Recognition of weeds at asparagus fields using multi-feature fusion and backpropagation neural network

Yafei Wang[1,2], Xiaodong Zhang[1,2], Guoxin Ma[1,2], Xiaoxue Du[1,2], Naila Shaheen[3], Hanping Mao[1,2*]

(1. *School of Agricultural Engineering, Jiangsu University, Zhenjiang 212013, China*;
2. *Key Laboratory of Modern Agricultural Equipment and Technology, Ministry of Education, Jiangsu University, Zhenjiang 212013, Jiangsu, China*;
3. *School of Electrical and Information Engineering, Jiangsu University, Zhenjiang 212013, Jiangsu, China*)

Abstract: In order to solve the problem of low recognition rates of weeds by a single feature, a method was proposed in this study to identify weeds in Asparagus (*Asparagus officinalis* L.) field using multi-feature fusion and backpropagation neural network (BPNN). A total of 382 images of weeds competing with asparagus growth were collected, including 135 of *Cirsium arvense* (L.) Scop., 138 of *Conyza sumatrensis* (Retz.) E. Walker, and 109 of *Calystegia hederacea* Wall. The grayscale images were extracted from the RGB images of weeds using the 2G-R-B factor. Threshold segmentation of the grayscale image of weeds was applied using Otsu method. Then the internal holes of the leaves were filled through the expansion and corrosion morphological operations, and other interference targets were removed to obtain the binary image. The foreground image was obtained by masking the binary image and the RGB image. Then, the color moment algorithm was used to extract weeds color feature, the gray level co-occurrence matrix and the Local Binary Pattern (LBP) algorithm was used to extract weeds texture features, and seven Hu invariant moment features and the roundness and slenderness ratio of weeds were extracted as their shape features. According to the shape, color, texture, and fusion features of the test samples, a weed identification model was built. The test results showed that the recognition rate of *Cirsium arvense* (L.) Scop., *Calystegia hederacea* Wall. and *Conyza sumatrensis* (Retz.) E. Walker were 82.72% (color feature), 72.41% (shape feature), 86.73% (texture feature) and 93.51% (fusion feature), respectively. Therefore, this method can provide a reference for the study of weeds identification in the asparagus field.

Keywords: weeds recognition, image processing, feature extraction, multi-feature fusion, BP neural network, asparagus field
DOI: 10.25165/j.ijabe.20211404.6135

Citation: Wang Y F, Zhang X D, Ma G X, Du X X, Shaheen N, Mao H P. Recognition of weeds at asparagus fields using multi-feature fusion and backpropagation neural network. Int J Agric & Biol Eng, 2021; 14(4): 190–198.

1 Introduction

Asparagus (*Asparagus Officinalis* L.), a perennial herb, is originated from the eastern Mediterranean and Asia Minor and has been cultivated for more than 2000 years, with the reputation of "the king of vegetables" in the international market. At present, asparagus is grown in more than sixty countries around the world, including the United States, Italy, Netherlands, Canada, Germany, and other countries. Its health benefits and biological functions have attracted increasing interest from both public and academia[1,2]. Currently, production, scientific research & development of Asparagus have extended from the developed to developing countries, and China is the largest country in cultivation and export of asparagus which accounts for over 90% of the global planting area of Asparagus[3,4]. However, in the growth of Asparagus, weeds play a significant role in limiting its crop productivity. They reduce crop yields by competition for resources and inhibition from allelopathic compounds[5-8]. Therefore, it is essential to explore effective weed identification strategies to ensure high crop yield.

Nowadays, the most common way of removing weeds is by spraying the herbicide uniformly all over the farmland. The areas without weeds are also sprayed, which increases the risk of contamination of crops, humans, animals, and water resources[9]. Herbicide-based control methods are playing a major role in weed control[10,11]. However, excessive use of herbicides can easily cause environmental pollution. These challenges emerge from a lack of attention on how weeds interact with the agroecosystem[12,13]. Machine vision technology has been suggested in precision agriculture for weed control[14]. This technique enables herbicides to be only sprayed at the exact spots needed. Thus, the effective identification of weeds is the foundation in precise control of weeds[15]. In order to solve this problem, the multi-feature fusion method based on machine vision can be used to identify weeds and spray them with pesticides[16].

Weed identification is mainly realized using machine vision technology via extracting their texture, color, and shape features[17-19]. The shape feature is extracted from a normalized description of the outline, whereas the texture and margin feature often use histogram accumulation of the leaf species. Scientists attempted to use different classifiers with different leaf features to solve it. Zhang et al.[20,21] evaluated ten common classifiers:

Received date: 2020-09-01 **Accepted date:** 2021-06-15
Biographies: Yafei Wang, PhD candidate, research interest: intelligent agricultural equipment and technology, Email: wangyafei918@126.com; **Xiaodong Zhang**, PhD, Associate Researcher, research interest: intelligent agricultural equipment and technology, Email: zxd700227@126.com; **Guoxin Ma**, PhD candidate, research interest: intelligent agricultural equipment and technology, Email: Gavin_Ma123@163.com; **Xiaoxue Du**, PhD candidate, research interest: intelligent agricultural equipment and technology, Email: dx66610474@163.com; **Naila Shaheen**, Master candidate, research interest: intelligent agricultural equipment and technology, Email: Naila Shaheen10@yahoo.com.
***Corresponding author: Hanping Mao**, PhD, Professor, research interest: modern agricultural equipment and environmental control technology of facility agriculture. Department of Agricultural Equipment, Jiangsu University, Zhenjiang, 212013, Jiangsu, China. Email: maohpujs@163.com.

k-Nearest Neighbors (KNN), support vector machine (SVM), nu-SVM, decision tree, random forest, naïve Bayes, linear discriminant analysis (LDA), logistic regression, quadratic discriminant analysis (QDA), and sparse representation in leaf species classification with different leaf features such as shape, texture, and margin. Sajad et al.[22] identified potato plants and three different kinds of weeds. By applying the image processing technique, 3459 samples were extracted, trained, and tested using neural network classifiers. One hundred twenty-six color features and sixty texture features were extracted from each sample. The experimental results showed that the proposed system achieved an excellent identification accuracy of 98.38%, requiring less than 0.8 s of execution on an average PC. Radhika et al.[23] used texture features extracted from Laws' texture masks for discrimination of carrot crops and weeds in digital images. A total of seventy texture features were extracted. The dimensionality reduction technique was used to get the optimal features. These features were used to train the Random Forest classifier. The results and observations from the experiment showed that the classifier achieved above 94% accuracy. Gai et al.[24] investigated fusion of color images and depth images. The results showed the fusion of color and depth was proved beneficial to the segmentation of crop plants from the background, which improved the average segmentation success rates from 87.2% (depth-based) and 76.4% (color-based) to 96.6% for broccoli, and from 74.2% (depth-based) and 81.2% (color-based) to 92.4% for lettuce, respectively. Farooq et al.[25] improved the separability of weeds by extracting the strength, texture, and shape characteristics of different categories of weeds. Dadashzadeh et al.[26] identified the discrimination of the rice and weeds, with a total of 302 color, shape, and texture features. Tang et al.[27] took the soybean seedlings and their associated weeds as the research object, and constructed a weed identification model based on *K*-means feature learning and combined with CNN. The experimental results have shown that this method with K-means pre-training achieved 92.89% accuracy, beyond 1.82% than CNN with random initialization and 6.01% than two layers network without fine-tuning.

The row spacing of asparagus planting is 1.2-1.5 m, and the plant spacing is 25-30 cm. It is easy to breed weeds between the lines, mainly including *Chenopodium album* L., *Calystegia hederacea* Wall., *Cirsium arvense* (L.) Scop., *Conyza sumatrensis* (Retz.) E. Walker, *Digitaria sanguinalis* (L.) Scop., *Echinochloa crusgalli* (L.) Beauv. and *Setaria viridis* (L.) Beauv., etc. Cirsium arvense (L.) Scop., *Calystegia hederacea* Wall. and *Conyza sumatrensis* (Retz.) E. Walker are perennial weeds, and are spread by seeds. They can spread quickly in open fields and have strong adaptability to the environment. The planting conditions of asparagus provide a favorable living space for these weeds, and the pesticides sprayed when planting asparagus is mostly for annual weeds, which are not effective for perennial weeds. The existing methods are based on one or two kinds of the three distinct characteristics in leaf images, including leaf contours, textures, and veins, which limits their recognition performance and scope of application[28]. Multi-feature fusion can help distinguish weeds, crops, and backgrounds, which improves the identification accuracy of weeds[29,30].

Therefore, the objective of this study was to classify *Cirsium arvense* (L.) Scop., *Calystegia hederacea* Wall. and *Conyza sumatrensis* (Retz.) E. Walker. First of all, the color moment algorithm was used to extract weeds color features, the gray level co-occurrence matrix (GLCM) and the Local Binary Pattern (LBP) algorithm were used to extract weeds texture features, seven Hu invariant moment features and the roundness and slenderness ratio of weeds were extracted as their shape features. Then, a method based on multi-feature fusion and backpropagation neural network (BPNN) was proposed to identify weeds in asparagus field.

2 Materials and methods

2.1 Image acquisition and pre-processing

2.1.1 Image acquisition

In this study, the experimental images were taken from the asparagus base in Shangcai County, Henan Province, China. The county is located in the region of 114°06′E-114°42′E and 33°04′N-33°25′N. The county has a flat terrain, deep soil layers, a warm temperate monsoon humid climate, abundant rainfall (average annual rainfall of 870.7 mm), moderate light (average yearly sunshine duration of 2089 h), long frost-free period (average frost-free period of 225 d), and distinct seasons (average annual temperature 14.7°C), which is suitable for asparagus cultivation. Experimental images were taken from March 20 to April 18, 2020. In order to fully consider the weather conditions of natural scenes, images were collected on sunny and cloudy days, respectively. In order to make the acquired images more representative, the overhead shooting method was adopted, and the shooting distance was 20-40 cm from the weeds. The acquisition equipment is Huawei nova5 Pro smartphone, the rear camera resolution of the mobile phone is 48 million pixels. A total of 382 images of weeds competing with asparagus growth were collected, including 135 images of *Cirsium arvense* (L.) Scop., 138 images of *Conyza sumatrensis* (Retz.) E. Walker, and 109 images of *Calystegia hederacea* Wall. These images were used in the training and testing of the weeds identification model. The experimental sample images are shown in Figure 1.

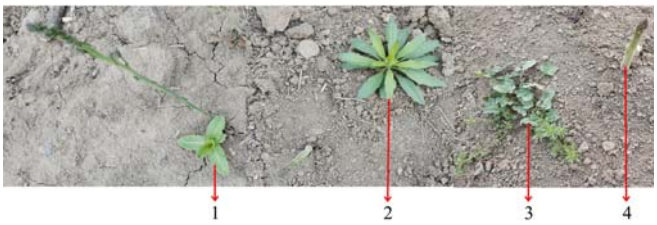

1. *Cirsium arvense* (L.) Scop. 2. *Conyza sumatrensis* (Retz.) E. Walker
3. *Calystegia hederacea* Wall. 4. *Asparagus officinalis* L.

Figure 1 Weeds images in the asparagus filed

2.1.2 Image pre-processing

Images were collected in the natural environment of the field. The background and lighting were different during image capture. The background includes dirt, shadows, dried weeds, and dried Asparagus stalks. Light conditions include direct sunlight and oblique radiation. Therefore, in order to highlight the green features of weeds, RGB image background should be removed. Equation (1) was used to convert RGB image (as shown in Figures 2a, 3a, and 4a) and obtain their grayscale image (as shown in Figures 2b, 3b, and 4b). In Equation (1), CF(x, y) is the gray value of the pixel coordinate (x, y), and R, G, and B represent the red, green, and blue color components of the pixel, respectively. Threshold segmentation of the grayscale image of weeds was applied using Otsu method. Then the internal holes of the leaves were filled through the expansion and corrosion morphological operations, and other interference targets were removed to obtain the binary images (as shown in Figures 2c, 3c, and 4c). The

foreground images were obtained by masking the binary image and the RGB image. The results are shown in Figures 2d, 3d, and 4d.

$$CF(x,y)=\begin{cases}0 & 2G-R-B<0\\ 2G-R-B & \text{Others}\\ 255 & 2G-R-B>255\end{cases} \quad (1)$$

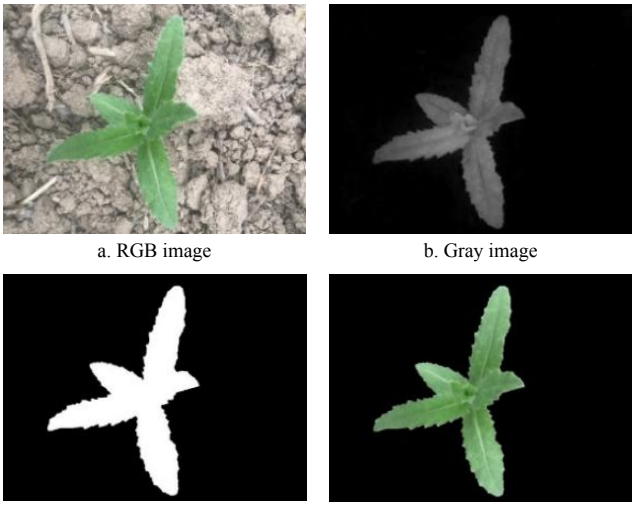

a. RGB image b. Gray image

c. Binary image d. Foreground image

Figure 2 Image segmentation of *Cirsium arvense* (L.) Scop.

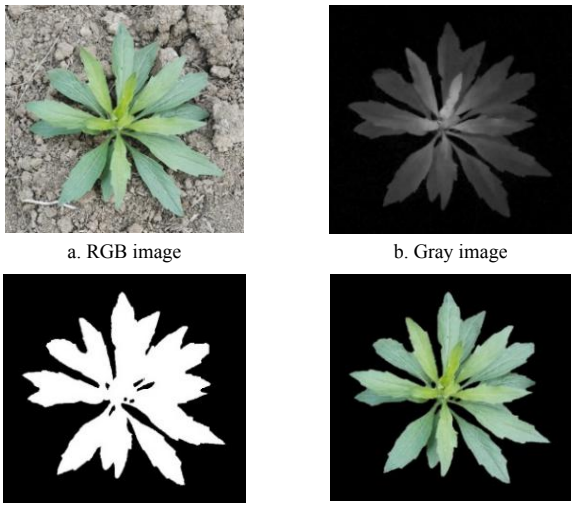

a. RGB image b. Gray image

c. Binary image d. Foreground image

Figure 3 Image segmentation of *Conyza sumatrensis* (Retz.) E. Walker

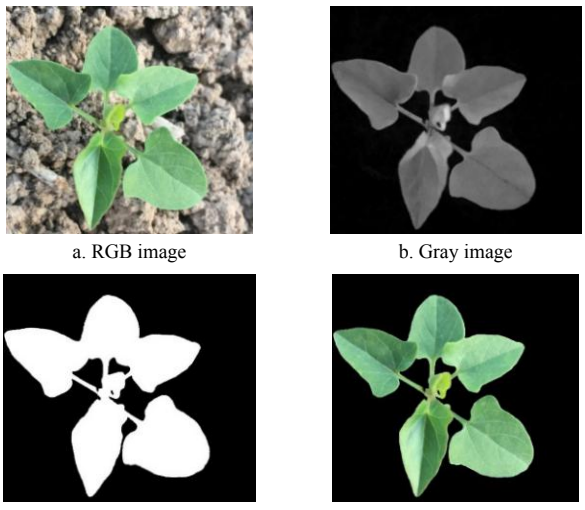

a. RGB image b. Gray image

c. Binary image d. Foreground image

Figure 4 Image segmentation of *Calystegia hederacea* Wall.

2.2 Feature extraction

In this study, in order to improve the accuracy and effectiveness of weed identification, the color, texture, and shape features of the weed images were extracted.

2.2.1 Color features

Color features were extracted based on pixels of images which has the advantages of stable features after rotation, scale, and translation changes. Since the colors of the three weeds are all green, the R, G, and B color component values of their RGB images have considerable overlap. The color moment can reflect the color distribution characteristics of the images, and the color moment feature in the statistical color feature can be analyzed to improve the recognition ability of the feature.

The HSV color space model was converted from the RGB color space model, which can be used for color expression in machine vision and as a supplement to the color features of weed images. However, the V component of the HSV color model is independent of color. In this study, only the color moment features of the R, G, B, H, and S components (mean, variance and skewness) were extracted under the RGB and HSV color space models of weed images, for a total of fifteen color features. The calculations were carried out by Equations (2)-(4).

$$\mu_i=\frac{1}{N}\sum_{j=1}^{N}P_{ij} \quad (2)$$

$$\sigma_i=\left[\frac{1}{N}\sum_{j=1}^{N}(P_{ij}-\mu_i)^2\right]^{\frac{1}{2}} \quad (3)$$

$$\xi_i=\left[\frac{1}{N}\sum_{j=1}^{N}(P_{ij}-\mu_i)^3\right]^{\frac{1}{3}} \quad (4)$$

where, μ_i, σ_i and ξ_i are the mean, variance, and skewness of color, respectively; P_{ij} is the i-th color channel component of the j-th pixel. N represents the number of pixels in the image.

2.2.2 Shape features

Shape features are used to describe the shape parameters of objects and have a commendable correlation with human visual perception systems. Weeds have different shapes. In this study, seven Hu invariant moment[31,32] features and the roundness and slenderness ratio of weeds were selected as their shape features. The calculation methods of roundness and sheer length are shown in Equations (5) and (6), respectively.

1) Form factor

$$\text{Form factor}=4\pi\frac{\text{Area}}{\text{Perimeter}^2} \quad (5)$$

where, Area represents the area of the target (total number of pixels); Perimeter represents the perimeter of the target, which is the outermost contour length of the target.

2) Eiongatedness

$$\text{Eiongatedness}=\frac{\text{Area}}{\text{Thickness}^2} \quad (6)$$

where, Thickness represents the width of the smallest circumscribed rectangle of the target.

2.2.3 Texture features

The surface properties of the scene corresponding to the image or image area were described by texture feature. It is a value calculated from the image. This value quantifies the characteristics of the gray level change within the image area. The texture feature of weed images belongs to the combination of regular texture and random texture.

At present, image texture feature extraction methods including

grayscale difference statistics, auto-correlation function, gray-level co-occurrence matrix (GLCM), local binary patterns (LBP) and spectrum-based feature analysis method[25,33]. Statistics-based texture analysis is the most common and most studied method in texture extraction methods[34]. In this study, the gray level co-occurrence matrix and local binary mode were selected, and the two texture features were fused as the texture features of the weeds images.

1) GLCM

Bhunia et al.[35] studied various statistical features in GLCM, and got four critical features of GLCM through experiments: Contrast, Asm, Entropy and Correlation. The GLCM should be normalized before calculation. The calculation equations are shown as Equations (7)-(11).

$$P_{\varphi,d}(i,j)=\frac{G_{\mathrm{GLCM}}(i,j)}{\sum_{i=0}^{N-1}\sum_{j=0}^{N-1}G_{\mathrm{GLCM}}(i,j)} \tag{7}$$

$$\mathrm{Contrast}=\sum_{i=0}^{N-1}\sum_{j=0}^{N-1}|i-j|^2\,P_{\varphi,d}(i,j) \tag{8}$$

$$\mathrm{Asm}=\sum_{i=0}^{N-1}\sum_{j=0}^{N-1}P_{\varphi,d}^2(i,j) \tag{9}$$

$$\mathrm{Entropy}=-\sum_{i=0}^{N-1}\sum_{j=0}^{N-1}P_{\varphi,d}(i,j)\log_2 P_{\varphi,d}(i,j) \tag{10}$$

$$\mathrm{Correlation}=\frac{\sum_{i=0}^{N-1}\sum_{j=0}^{N-1}\left[(i,j)P_{\varphi,d}(i,j)-\mu_x\mu_y\right]}{\sigma_x\sigma_y} \tag{11}$$

where, $P_{\varphi,d}(i,j)$ is the normalized gray-level co-occurrence matrix; $G_{\mathrm{GLCM}}(i,j)$ is the original gray-level co-occurrence matrix.

$$\mu_x=\sum_{i=0}^{N-1}i\sum_{j=0}^{N-1}P_{\varphi,d}(i,j) \tag{12}$$

$$\mu_y=\sum_{j=0}^{N-1}j\sum_{i=0}^{N-1}P_{\varphi,d}(i,j) \tag{13}$$

$$\sigma_x^2=\sum_{i=0}^{N-1}(i-\mu_x)^2\sum_{j=0}^{N-1}P_{\varphi,d}(i,j) \tag{14}$$

$$\sigma_y^2=\sum_{j=0}^{N-1}(i-\mu_y)^2\sum_{i=0}^{N-1}P_{\varphi,d}(i,j) \tag{15}$$

In the experiment, the pre-processed images were converted into sixteen gray levels, and then four key features of GLCM in four directions (0°, 45°, 90°, and 135°) were calculated to obtain a total of sixteen feature values.

2) LBP

The LBP texture feature description method has the advantages of having simple principle, small calculation, grayscale invariance and rotation invariance[36]. It uses the difference between the gray value of the center pixel and the adjacent pixel to generate the LBP code. The basic symbols related to LBP were defined as follows: g_c represents the gray value of the center point of the local area, g_p (p=0, 1, …, 7) corresponds to the points distributed equally around the center point, (x_c, y_c) represents the center point coordinate. The LBP local area texture calculation equation centered on (x_c, y_c) are shown in Equations (16) and (17).

$$s(g_p-g_c)=\begin{cases}1 & g_p-g_c\ge 0\\ 0 & g_p-g_c<0\end{cases} \tag{16}$$

$$\mathrm{LBP}(x_c,y_c)=\sum_{p=0}^{7}s(g_p-g_c)2^p \tag{17}$$

The LBP operator with 8 points in the neighborhood can generate 2^8 kinds of LBP values, which determines the dimension of texture features. In order to solve the problem of too many binary modes and improve statistics, Kou et al[37] proposed the "equivalent mode" to reduces the dimension of the mode types of LBP operators. The adjacent elements from 0 to 1 or 1 to 0 were regarded as a transition. The value of the transition that did not exceed two during the calculation process was called the LBP equivalent mode, a total of 58 kinds, otherwise they are called the mixed mode. In this study, this method was used to change the binary mode from the original 256 dimensions to 59 dimensions.

2.3 Classification and identification of weeds using BP neural network

The BP neural network, which is also called the error reverse transmission neural network, is a neural network that uses the feedback values to adjust the connection between neurons continuously. A three-layer BP neural network that trained with the multi-feature fusion of weeds was used to evaluate the relationship between the combination of features and weeds. The specific steps were as follows.

1) Training and test samples

Three varieties of weeds, namely, *Cirsium arvense* (L.) Scop., *Conyza sumatrensis* (Retz.) E. Walker and *Calystegia hederacea* Wall. were selected as test samples, which have 135, 138, 109 samples, respectively (a total of 382 samples). Further, 70% of the samples were used as a training set to train the BP neural network, and the other samples were used to test the trained network model. The flowchart of the algorithm for weeds classification is shown in Figure 5.

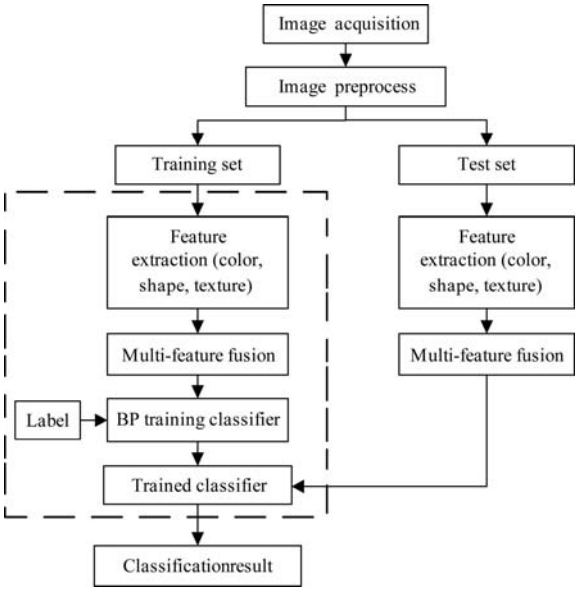

Figure 5 Process of weeds identification and classification

2) Hidden layer

The hidden layer of the BP neural network is crucial for overall network performance. The number of neurons in the hidden layer was selected according to $\sqrt{n_1\times n_2}+a$, where n_1 denotes the number of input parameters, n_2 denotes the number of output parameters, and $a\in[0, 10]$. Therefore, n_1 was defined as the input-vector dimension, while n_2 was defined as the output-vector dimension.

3 Results and discussion

The operating system for the entire test process is Windows 7,

and the development software is MATLAB 2016b and Python 3.8. A computer memory of 4 GB. Processor AMD A8-4555M APU with Radeon (TM) HD Graphics 1.6 GHz was used.

3.1 Results of feature extraction

In this study, the color moment algorithm was used to extract the mean, variance, and skewness of the R, G, B, H, and S color components, for a total of 15 color features. The gray level co-occurrence matrix and the LBP algorithm were used to extract 16 gray level co-occurrence matrices and 59 LBP features. Seven Hu invariant moment features and the roundness and slenderness ratio of weeds were extracted as their shape features. The feature extraction results are shown in Figures 6-8 and Table 1.

In order to eliminate the dimensional effects of weed eigenvalues, it needs to be normalized[36]. The normalized equation is shown in Equation (18).

$$x_i = 2 \times \frac{x_i - x_{\min}}{x_{\max} - x_{\min}} - 1 \tag{18}$$

where, x_i represents the eigenvalue element; $x_{\min}$ and $x_{\max}$ represent the minimum and maximum eigenvalue of elements, respectively. The normalized characteristic means are shown in Figure 9.

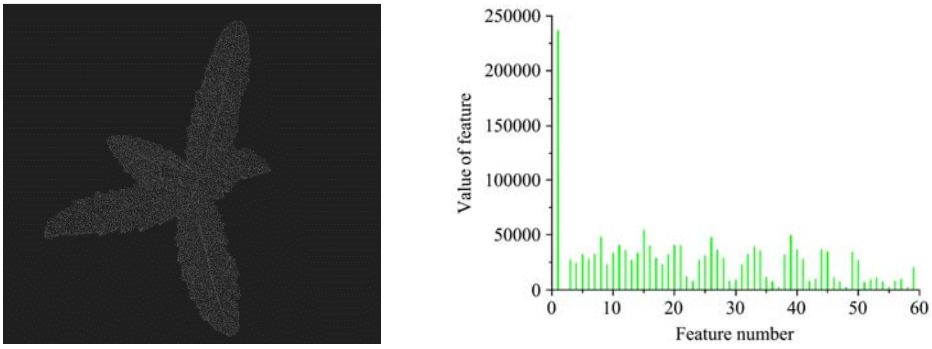

a. LBP feature image b. Feature value of LBP image

Figure 6 LBP feature for *Cirsium arvense* (L.) Scop.

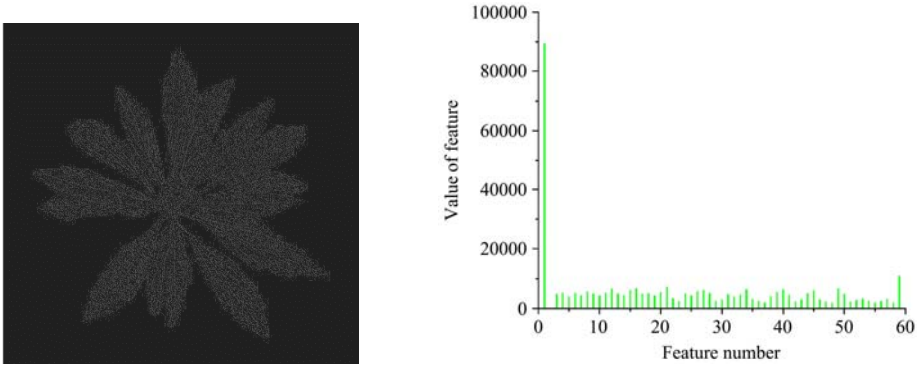

a. LBP feature image b. Feature value of LBP image

Figure 7 LBP feature for *Conyza sumatrensis* (Retz.) E. Walker

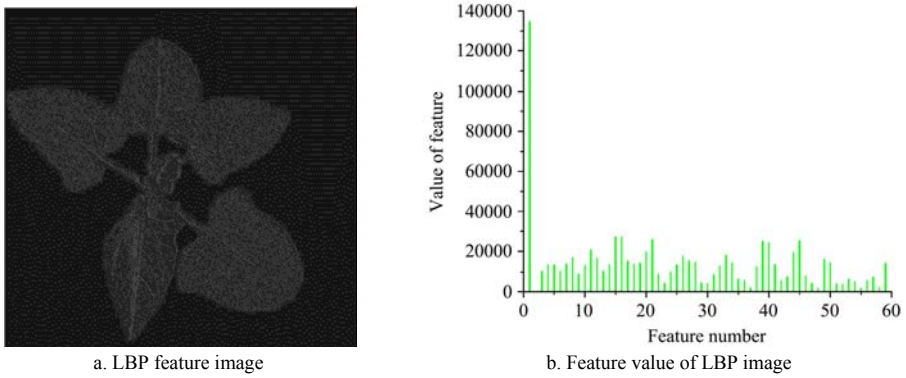

a. LBP feature image b. Feature value of LBP image

Figure 8 LBP feature for *Calystegia hederacea* Wall.

Table 1 Feature extraction results of weeds

Feature	Average value			Feature	Average value		
	Conyza sumatrensis (Retz.) E. Walker	*Calystegia hederacea* Wall.	*Cirsium arvense* (L.) Scop.		*Conyza sumatrensis* (Retz.) E. Walker	*Calystegia hederacea* Wall.	*Cirsium arvense* (L.) Scop.
R_mean	45.8667	42.7536	17.1309	Entropy (0°)	2.1593	2.1959	1.0375
G_mean	57.3106	61.5603	24.0253	Correlation (45°)	0.9820	0.9908	0.9944
B_mean	46.2091	43.5314	16.1198	Contrast (45°)	0.8261	0.4253	0.1081
H_mean	0.1253	0.1198	0.0470	Asm (45°)	0.4797	0.4644	0.7377
S_mean	0.1200	0.1324	0.0537	Entropy (45°)	2.2345	2.2481	1.0559

Feature	Average value			Feature	Average value		
	Conyza sumatrensis (Retz.) E. Walker	*Calystegia hederacea* Wall.	*Cirsium arvense* (L.) Scop.		*Conyza sumatrensis* (Retz.) E. Walker	*Calystegia hederacea* Wall.	*Cirsium arvense* (L.) Scop.
R_variance	28.4164	27.0969	24.2520	Correlation (90°)	0.9873	0.9937	0.9964
G_variance	35.1287	36.9628	33.4291	Contrast (90°)	0.5831	0.2921	0.0709
B_variance	29.1671	27.1137	23.1441	Asm (90°)	0.4830	0.4668	0.7382
H_variance	0.0706	0.0658	0.0640	Entropy (90°)	2.1530	2.1560	1.0355
S_variance	0.0921	0.0836	0.0838	Correlation (135°)	0.9827	0.9915	0.9945
R_third moment	68.2413	64.4991	49.3987	Contrast (135°)	0.7898	0.3915	0.1065
G_third moment	82.6966	92.1044	66.6943	Asm (135°)	0.4801	0.4647	0.7377
B_third moment	67.5192	68.5994	48.4416	Entropy (135°)	2.2321	2.2371	1.0561
H_third moment	0.1706	0.2054	0.1299		5.3325	5.3205	4.2408
S_third moment	0.3107	0.2987	0.1763		10.8609	10.9009	8.6610
Form factor	0.0072	0.0168	0.0149		28.3732	25.4743	21.1588
Eiongatedness	0.5033	0.605	0.4532	Hu invariant moments	26.9369	26.5287	19.6618
Correlation (0°)	0.9881	0.9940	0.9960		26.0880	25.5443	18.5659
Contrast (0°)	0.5462	0.2783	0.0769		32.7587	32.1775	23.9954
Asm (0°)	0.4830	0.4661	0.7381		54.6419	52.7004	41.4980

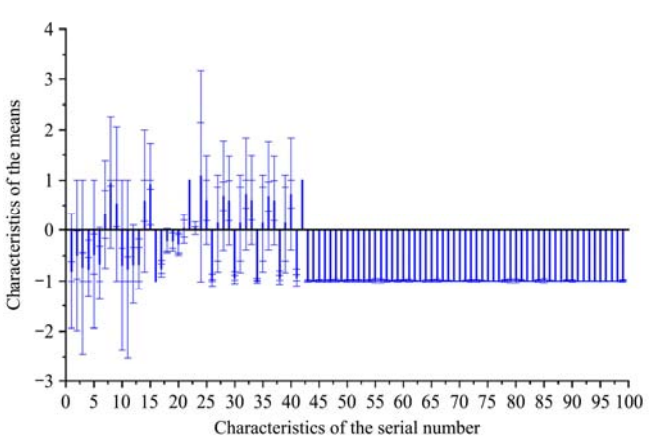

a. *Cirsium arvense* (L.) Scop.

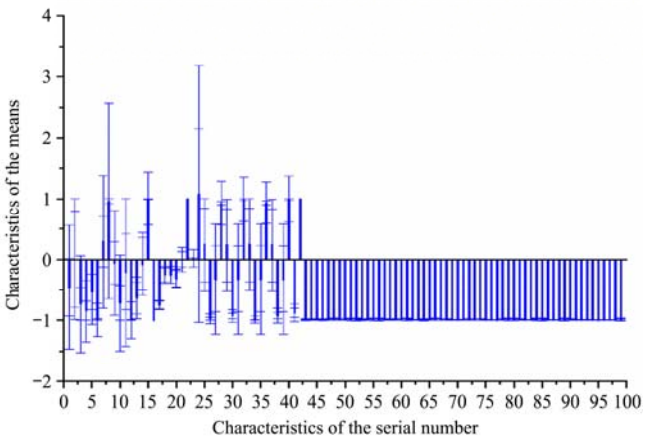

b. *Conyza sumatrensis* (Retz.) E. Walker

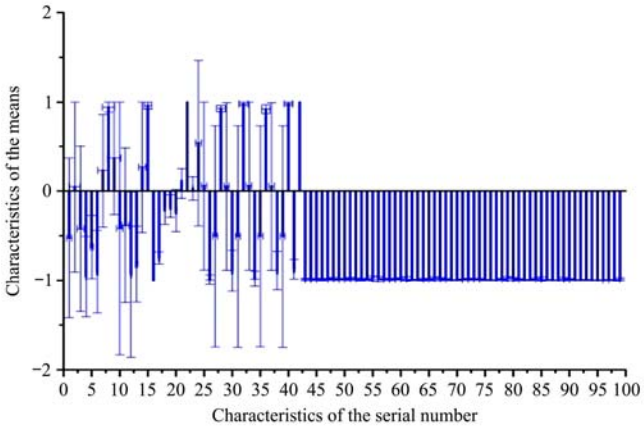

c. *Calystegia hederacea* Wall.

Figure 9 Normalized characteristics means of three weeds

3.2 Selection and analysis of weed features

Feature selection was the key to weed identification[38]. As shown in Figures 6-8 and Table 1 that the G_variance, H_variance, S_variance, Correlation at direction 0° 45°, 90°, and 135° and characteristics data of the three weeds are familiar. LBP features include 58 uniform patterns and other values (i.e., class 59)[39]. Therefore, in order to reduce computation and improve weed recognition speed, remove the characteristics data of G_variance, H_variance, S_variance, Correlation of directions 0°, 45°, 90°, 135°, and other values (i.e., class 59) of the LBP features.

Besides, the color features and texture features of weed *Cirsium arvense* (L.) Scop. were different from *Conyza sumatrensis* (Retz.) E. Walker, and *Calystegia hederacea* Wall., but the shape features were similar. Thus, in order to improve the recognition speed, color features and texture features were selected to distinguish *Cirsium arvense* (L.) Scop. from *Conyza sumatrensis* (Retz.) E. Walker, and *Calystegia hederacea* Wall. However, color feature, shape feature, texture feature about *Conyza*

sumatrensis (Retz.) E. Walker, and *Calystegia hederacea* Wall., were familiar. Therefore, in order to improve the recognition rate of *Conyza sumatrensis* (Retz.) E. Walker, and *Calystegia hederacea* Wall., color features, shape features, and texture features are needed to be integrated.

3.3 Results of weed identification

In this study, color features, shape features and texture features of weed images were extracted. The recognition models based on BPNN were built. The recognition rate and recognition rate time are shown in Table 2.

Table 2 Recognition rate and recognition time for BPNN

Name of weeds	Feature type	Feature number	Net (Input layer, Hidden layer, Output layer)	Recognition rate (BPNN)/%	Recognition time/s
Cirsium arvense (L.) Scop. and *Calystegia hederacea* Wall.	Color feature	12	(12, 6, 2)	81.38	1
	Texture feature	70	(70, 13, 2)	88.35	2
	Fusion feature	82	(82, 15, 2)	98.72	3
Cirsium arvense (L.) Scop. and *Conyza sumatrensis* (Retz.) E. Walker	Color feature	12	(12, 6, 2)	95.18	1
	Texture feature	70	(70, 13, 2)	86.34	3
	Fusion feature	82	(82, 15, 2)	97.59	4
Calystegia hederacea Wall. and *Conyza sumatrensis* (Retz.) E. Walker	Color feature	12	(12, 6, 2)	75.86	1
	Shape feature	9	(9, 5, 2)	89.61	1
	Texture feature	70	(70, 13, 2)	90.91	2
	Fusion feature	91	(91, 15, 2)	96.10	3
Cirsium arvense (L.) Scop., *Calystegia hederacea* Wall. and *Conyza sumatrensis* (Retz.) E. Walker	Color feature	12	(12, 8, 3)	82.72	3
	Shape feature	9	(9, 6, 3)	72.41	2
	Texture feature	70	(70, 16, 3)	86.73	6
	Fusion feature	91	(91, 18, 3)	93.51	8

As can be seen from Table 2, the recognition rate of *Cirsium arvense* (L.) Scop., and *Calystegia hederacea* Wall. was 81.38% (based on color feature), 88.35% (based on texture feature) and 98.72% (based on fusion feature), respectively. Moreover, the recognition time was 3 s based on the fusion feature. The recognition rate based on fusion feature was higher than that of color feature and texture feature. However, the recognition time was similar. Thus, fusion feature (color feature and texture feature) was selected when identifying *Cirsium arvense* (L.) Scop., and *Calystegia hederacea* Wall.

The recognition rate of *Cirsium arvense* (L.) Scop., and *Conyza sumatrensis* (Retz.) E. Walker was 95.18% (based on color feature), 86.34% (based on texture feature), and 97.59% (based on fusion feature), respectively. Recognition rates were similarly based on color feature and fusion feature, respectively. However, the recognition time based on color feature was lower than fusion feature. Thus, color feature was selected when identifying *Cirsium arvense* (L.) Scop., and *Conyza sumatrensis* (Retz.) E. Walker.

The recognition rate of *Calystegia hederacea* Wall., and *Conyza sumatrensis* (Retz.) E. Walker was 75.86% (based on color feature), 89.61% (based on shape feature), 90.91% (based on texture feature), and 96.10% (based on fusion feature), respectively. Furthermore, the recognition time was 3 s based on fusion feature. The recognition rate based on feature fusion was higher than that of color feature, shape feature, and texture feature. Otherwise, the recognition time was similar. Thus, fusion feature (color feature, shape feature, and texture feature) was selected when identifying *Calystegia hederacea* Wall, and *Conyza sumatrensis* (Retz.) E. Walker.

The recognition rate of *Cirsium arvense* (L.) Scop., *Calystegia hederacea* Wall., and *Conyza sumatrensis* (Retz.) E. Walker was 82.72% (based on color feature), 72.41% (based on shape feature), 86.73% (based on texture feature), and 93.51% (based on fusion feature), respectively. Moreover, the recognition time was 8 s based on fusion feature. It can meet the requirement of weed identification time[40]. The recognition rate based on fusion feature was higher than that of color feature, shape feature, and texture feature. Thus, fusion feature (color feature, shape feature, and texture feature) was selected when identifying *Cirsium arvense* (L.) Scop., *Calystegia hederacea* Wall., and *Conyza sumatrensis* (Retz.) E. Walker.

The recognition rate of *Cirsium arvense* (L.) Scop., *Calystegia hederacea* Wall. and *Conyza sumatrensis* (Retz.) E. Walker based on shape feature was lower than that of color feature and texture feature. The morphology of *Cirsium arvense* (L.) Scop., and *Conyza sumatrensis* (Retz.) E. Walker may be similar because *Cirsium arvense* (L.) Scop., and *Conyza sumatrensis* (Retz.) E. Walker belong to the composite family, but color feature and texture were different among the different family and genus[41]. However, the recognition rates of color feature, shape feature, and texture feature were all lower than that based on multi-feature fusion. That is because multi-feature fusion contains more weed image information so that it can improve the identification accuracy of weeds[29].

In addition, in this study, the recognition rates of different recognition models based on the multi-feature fusion were compared. Based on these features, *K*-Nearest Neighbor (KNN), Random Forest (RF), and Support Vector Machine (SVM) recognition models were built. The hyper-parameter *K* of the KNN algorithm was set to 4. The number of RF model trees was set to 100. The minimum sample required to split the internal nodes was set to 2. The minimum number of samples on the leaf node of the RF algorithm was set to 1. The SVM algorithm used Gaussian kernel function, and the recognition method used one-vs-one[33]. The recognition rate for weeds using the BPNN model was 93.51%, while the recognition rate of the KNN, RF, and SVM models were 89.56%, 84.92%, and 92.67%, respectively. BPNN model has the best recognition performance.

4 Conclusions

In this study, according to the characteristics of the weeds at

asparagus fields, 2G-R-B color factors were used to convert RGB images of weeds to grayscale images. Threshold segmentation of the grayscale image of weeds was applied using Otsu method. Then the internal holes of the leaves were filled through the expansion and corrosion morphological operations, and other interference targets were removed to obtain the binary image. The foreground image was obtained by masking the binary image and the RGB image. Then, the color moment algorithm was used to extract weeds color feature, the gray level co-occurrence matrix and the LBP algorithm were used to extract weeds texture features, and seven Hu invariant moment features and the roundness and slenderness ratio of weeds were extracted as their shape features. Recognition rates of *Cirsium arvense* (L.) Scop., and *Calystegia hederacea* Wall. were 81.38% (based on color feature), 88.35% (based on texture feature) and 98.72% (based on fusion feature), respectively. Recognition rates of *Cirsium arvense* (L.) Scop, and *Conyza sumatrensis* (Retz.) E. Walker were 95.18% (based on color feature), 86.34% (based on texture feature), and 97.59% (based on fusion feature), respectively. Recognition rates of *Calystegia hederacea* Wall, and *Conyza sumatrensis* (Retz.) E. Walker, were 75.86% (based on color feature), 89.61% (based on shape feature), 90.91% (based on texture feature), and 96.10% (based on fusion feature), respectively. Recognition rates of *Cirsium arvense* (L.) Scop., *Calystegia hederacea* Wall., and *Conyza sumatrensis* (Retz.) E. Walker were 82.72% (based on color feature), 72.41% (based on shape feature), 86.73% (based on texture feature), and 93.51% (based on fusion feature), respectively.

In future work, the authors plan to obtain more data sets and use a deep learning framework for weed classification to obtain better classification results. Furthermore, since more images will be added to the provided dataset, more experiments will be performed in order to always deploy the best weed identification system.

Acknowledgements

This work was partially supported by the National Natural Science Foundation of China (Grant No. 32071905; No. 61771224); the National Key Research and Development Plan of China (Grant No. 2018YFF0213601); the National Natural Science Foundation of China (Grant No. 61771224); the Jiangsu Demonstration Project of Modern Agricultural Machinery Equipment and Technology (Grant No. NJ2019-19); the China Agriculture Research System (CARS-23-C03).

[References]

[1] Guo Q B, Wang N F, Liu H H, Li Z, Lu L F, Wang C L. The bioactive compounds and biological functions of *Asparagus officinalis* L.– A review. Journal of Functional Foods, 2020; 65: 103727. doi: 10.1016/ j.jff.2019.103727.

[2] Lwin W W, Srilaong V, Boonyaritthongchai P, Wongs A C, Pongprasert N. Electrostatic atomized water particles reduce postharvest lignification and maintain saparagus quality. Scientia Horticulturae, 2020; 271: 109487. doi: 10.1016/j.scienta.2020.109487.

[3] Zhang J, Zhang F, Li D R, Liu Y C, Liu B J, Meng X H. Characterization of metabolite profiles of white and green spears of *Asparagus officinalis* L. from Caoxian, East China. Food Research International, 2020; 128: 108869. doi: 10.1016/j.foodres.2019.108869.

[4] Siomos A S. The quality of asparagus as affected by preharvest factors. Scientia Horticulturae, 2018; 233: 510–519.

[5] Pahikkala T, Kari K, Mattila H, Lepisto A, Teuhola J, Nevalainen O S, et al. Classification of plant species from images of overlapping leaves. Computers and Electronics in Agriculture, 2015; 118: 186–192.

[6] Miao R H, Tang J L, Chen X Q. Classification of farmland images based on color features. J. Visual Commun. Image Represent, 2015; 29: 138–146.

[7] Rehman T U, Zaman Q U, Chang Y K, Schumann A W, Corscadden K W, Esau T J. Optimising the parameters influencing performance and weed (goldenrod) identification accuracy of colour co-occurrence matrices. Biosystems Engineering, 2018; 170: 85–95.

[8] Li H, Travlos I, Qi L J, Kanatas P, Wang P. Optimization of herbicide use: Study on spreading and evaporation characteristics of glyphosate-organic silicone mixture droplets on weed leaves. Agronomy-Basel, 2019; 9(9): 547. doi: 10.3390/agronomy9090547.

[9] Van Bruggen A H C, He M M, Shin K, Mai V, Jeong K C, Finckh M R, et al. Environmental and health effects of the herbicide glyphosate. Science of the Total Environment, 2018; 616-617: 255–268.

[10] Zhu J W, Wang J, DiTommaso A, Zhang C X, Zheng G P, Liang W, et al. Weed research status, challenges, and opportunities in China. Crop Protection, 2020; 134: 104449. doi: 10.1016/j.cropro.2018.02.001.

[11] Ullah R, Aslam Z, Maitah M, Zaman Q, Bashir S, Hassan W, et al. Sustainable weed control and enhancing nutrient use efficiency in crops through Brassica (*Brassica compestri*s L.) allelopathy. Sustainability, 2020; 12(14): 5763. doi:10.3390/su12145763.

[12] MacLaren C, Storkey J, Menegat A, Metcalfe H, Dehnen-Schmutz K. An ecological future for weed science to sustain crop production and the environment. A review. Agronomy for Sustainable Development, 2020; 40(4): 24. doi: 10.1007/s13593-020-00631-6.

[13] Caser M, Demasi S, Caldera F, Dhakar N K, Trotta F, Scariot V. Activity of *Ailanthus altissima* (Mill.) swingle extract as a potential bioherbicide for sustainable weed management in horticulture. Agronomy, 2020; 10(7): 965. doi: 10.3390/agronomy10070965.

[14] Pannacci E, Farneselli M, Guiducci M, Tei F. Mechanical weed control in onion seed production. Crop protection, 2020; 135: 105221. doi: 10.1016/j.cropro.2020.105221.

[15] Molinari F A, Blanco A M, Vigna M R, Chantre G R. Towards an integrated weed management decision support system: A simulation model for weed-crop competition and control. Computers and Electronics in Agriculture, 2020; 175: 105597. doi: 10.1016/j.compag.2020.105597.

[16] Nichols V, Verhulst N, Cox R, Govaerts B. Weed dynamics and conservation agriculture principles: A review. Field Crops Research, 2015; 183: 56–68.

[17] Qiao X, Li Y Z, Su G Y, Tian H K, Zhang S, Sun Z Y, et al. MmNet: Identifying *Mikania micrantha* Kunth in the wild via a deep Convolutional Neural Network. Journal of Integrative Agriculture, 2020; 19(5): 1292–1300.

[18] Borja E G, Nikos M, Loukas A, Spyros F, Ioannis V. Towards weeds identification assistance through transfer learning. Computers and Electronics in Agriculture, 2020; 171: 105306. doi: 10.1016/j.compag.2020.105306.

[19] Favreliere E, Ronceux A, Pernel J, Meynard J M. Nonchemical control of a perennial weed, *Cirsium arvense*, in arable cropping systems. A review. Agronomy for Sustainable Development, 2020; 40(4): 31. doi: 10.1007/s13593-020-00635-2.

[20] Zhang Q, Zeng S N, Zhang B B. Initial investigation of different classifiers for plant leaf classification using multiple features. In: Proceedings of Eleventh International Conference on Digital Image Processing (ICDIP), Guangzhou, 2019; pp.256–264. doi: 10.26914/c.cnkihy.2019.007593.

[21] Zeng S N, Zhang B B, Du Y. Joint distances by sparse representation and locality-constrained dictionary learning for robust leaf recognition. Computers and Electronics in Agriculture, 2017; 142(Part B): 563–571.

[22] Sajad S, Yousef A G, Ginés G M. A fast and accurate expert system for weed identification in potato crops using metaheuristic algorithms. Computers in Industry, 2018; 98: 80–89.

[23] Radhika K, Mamatha B, Srikanth P. Crop and weed discrimination using Laws' texture masks. Int J Agric & Biol Eng, 2020; 13(1): 191-197.

[24] Gai J Y, Tang L, Stewad B L. Automated crop plant detection based on the fusion of color and depth images for robotic weed control. Journal of Field Robotics, 2020; 37(1): 35–52.

[25] Farooq A, Jia X P, Hu J K, Zhou J. Multi-resolution weed classification via convolutional neural network and superpixel based local binary pattern using remote sensing image. Remote Sensing, 2019; 11(14): 1692. doi: 10.3390/rs11141692.

[26] Dadashzadeh M, Abbaspour-Gilandeh Y, Mesri-Gundoshmian T, Sabzi S, Hernandez-Hernandez J L, Hernandez-Hernandez M, et al. Weed classification for site-specific weed management using an automated stereo

computer-vision machine-learning system in rice fields. Plants-basel, 2020; 9(5): 559. doi: 10.3390/plants9050559.

[27] Tang J L, Wang D, Zhang Z G, He L J, Xin J, Xu Y. Weed identification based on K-means feature learning combined with convolutional neural network. Computers and Electronics in Agriculture, 2017; 135: 63-70.

[28] Wang X, Du W K, Hu S M. Leaf recognition based on elliptical half Gabor and maximum gap local line direction pattern. IEEE Access, 2020; 8: 39175–39183.

[29] Aakif A, Khan M F. Automatic classification of plants based on their leaves. Biosystems Engineering, 2015; 139: 66–75.

[30] Bester T M, Timothy D, Saliou N, Emily K, Tobias L, Zeyaur K, et al. Is it possible to discern Striga weed (Striga hermonthica) infestation levels in maize agro-ecological systems using in-situ spectroscopy? Int J Appl Earth Obs Geoinformation, 2020; 85: 102008. doi: 10.1016/j.jag.2019.102008.

[31] Wang A C, Zhang W, Wei X H. A review on weed detection using ground-based machine vision and image processing techniques. Computers and Electronics in Agriculture, 2019; 158: 226–240.

[32] Bosili P, Duckett T, Cielniak G. Analysis of morphology-based features for classification of crop and weeds in precision agriculture. IEEE Robotics and Automation Letters, 2018; 3(4): 295–1956.

[33] Wang Y F, Du X X, Ma G X, Liu Y, Wang B, Mao H P. Classification methods for airborne disease spores from greenhouse crops based on multifeature fusion. Applied Science, 2020; 10(21): 7850. doi: 10.3390/app10217850.

[34] Deng X W, Qi L, Ma X, Jiang Y, Chen X S, Liu H Y, et al. Recognition of weeds at seedling stage in paddy fields using multi-feature fusion and deep belief networks. Transactions of the CSAE, 2018; 34(14): 165–172. (in Chinese)

[35] Bhunia A K, Bhattacharyya A, Banerjee P. A noval feature descriptor for image retrieval by combining modified color histogram and diagonally symmetric co-occurrence texture pattern. Pattern Analysis and Applications, 2020; 23: 703–723.

[36] Liu L, Fieguth P, Guo Y L, Wang X G, Pietikäinen M. Local binary features for texture classification: Taxonomy and experimental study. Pattern Recognition, 2017; 62: 135–160.

[37] Kou Q Q, Cheng D Q, Chen L L, Zhao K. A multiresolution gray-scale and rotation invariant descriptor for texture classification. IEEE Access, 2018; 6: 30691–30701.

[38] Lauwers M, Cauwer B D, Nuyttens D, Cool S R, Pieters J G. Hyperspectral classification of *Cyperus esculentus* clones and morphologically similar weeds. Sensors, 2020; 20(9): 2504. doi: 10.3390/s20092504.

[39] Deng X W, Qi L, Ma X, Jiang Y, Chen X S, Liu H Y, et al. Recognition of weeds at seedling stage in paddy fields using multi-feature fusion and deep belief networks. Transactions of the CSAE, 2018; 34(14): 165–172. (in Chinese)

[40] Xu K, Li H M, Cao W X, Zhu Y, Chen R J, Ni J. Recognition of weeds in wheat fields based on the fusion of RGB images and depth images. IEEE Access, 2020; 8: 110362–110370.

[41] Thyagharajan K K, Raji I K. A review of visual descriptors and classification techniques used in leaf species identification. Archives of Computational Methods in Engineering, 2019; 26: 933–960.